THE JOURNAL OF PHYSICAL CHEMISTRY A

Article

pubs.acs.org/JPCA

Effect of Water on Hydrolytic Cleavage of Non-Terminal α-Glycosidic Bonds in Cyclodextrins To Generate Monosaccharides and Their Derivatives in a Dimethyl Sulfoxide−Water Mixture

Hiroshi Kimura,[†] Masaki Hirayama,[†] Ken Yoshida,*[,†] Yasuhiro Uosaki,[†] and Masaru Nakahara[‡]

[†]Department of Chemical Science and Technology, Faculty of Engineering, University of Tokushima, 2-1 Minamijosanjima-cho, Tokushima 770-8506, Japan

[‡]Institute for Chemical Research, Kyoto University, Uji, Kyoto 611-0011, Japan

Supporting Information

ABSTRACT: Hydrolytic cleavage of the non-terminal α-1,4-glycosidic bonds in α-, β-, and γ-cyclodextrins and the anomeric-terminal one in D-maltose was investigated to examine how the cleavage rate for α-, β-, and γ-cyclodextrins is slower than that for D-maltose. Effects of water and temperature were studied by applying in situ ^{13}C NMR spectroscopy and using a dimethyl sulfoxide (DMSO)−water mixture over a wide range of water mole fraction, x_w = 0.004−1, at temperatures of 120−180 °C. The cleavage rate constant for the non-anomeric glycosidic bond was smaller by a factor of 6−10 than that of the anomeric-terminal one. The glycosidic-bond cleavage is significantly accelerated through the keto−enol tautomerization of the anomeric-terminal D-glucose unit into the D-fructose one. The smaller the size of the cyclodextrin, the easier the bond cleavage due to the ring strain. The remarkable enhancement in the cleavage rate with decreasing water content was observed for the cyclodextrins and D-maltose as well as D-cellobiose. This shows the important effect of the solitary water whose hydrogen bonding to other water molecules is prohibited by the presence of the organic dipolar aprotic solvent, DMSO, and which has more naked partial charges and higher reactivity. A high 5-hydroxymethyl-2-furaldehyde (5-HMF) yield of 64% was attained in a non-catalytic conversion by tuning the water content to x_w = 0.30, at which the undesired polymerization by-paths can be most effectively suppressed. This study provides a step toward designing a new optimal, earth-benign generation process of 5-HMF starting from biomass.

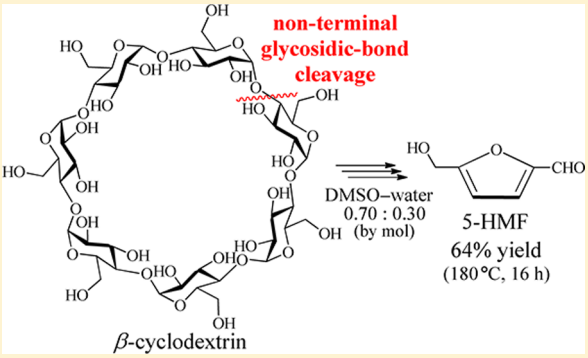

1. INTRODUCTION

Hydrolytic cleavage of the α- and β-glycosidic bonds is essential for the conversion of biomass-derived polysaccharides into valuable chemicals through the depolymerization. In our previous studies,[1−4] we have developed a non-catalytic method for the hydrothermal decomposition of oligosaccharides (di-, tri-, and tetraose) into a monosaccharide D-glucose and its dehydrated derivatives through the elimination of the anomeric-terminal D-glucose unit by monitoring the observable elementary processes using the in situ NMR. Also it has been found that the glycosidic-bond cleavage of D-cellobiose is remarkablly sensitive to the water content in DMSO−water mixtures.[4] In particular, a key role is played by the "solitary water" that is not hydrogen-bonded to other water molecules as in supercritical water clusters with the molecular partial charges more naked.[5−7] Toward the full understandings of the decomposition of biopolysaccharides whose glycosidic bonds are mostly non-terminal, light should also be shed on the cleavage of the non-terminal glycosidic bond as well as the anomeric-terminal one. We should ask to what extent the non-terminal cleavage is more difficult than the terminal one and why it is. For the purpose, we focus on cyclodextrins in the present study as the model substrate before going to substantially longer polymer chains. β-Cyclodextrin is composed of the seven-membered closed ring of D-glucose units linked by α-1,4-glycosidic bond and therefore contains only the non-terminal glycosidic bonds. Owing to its highly symmetric structure, the closed-ring and the open-ring heptamer produced by one glycosidic-bond cleavage can be distinghished from each other by ^{13}C NMR spectroscopy. This enables us to distinguish the cleavage position of glycosidic bond and to analyze the difference in the kinetics between the non-terminal and the anomeric-terminal glycosidic-bond cleavages, which has not been quantitatively discussed so far in the polysaccharide decomposition.[8−17] The α-1,4-glycosidic bond is the one involved in starch and malto-oligosaccharides, and thus the present study will lead to an insightful step toward the practical

Received: December 25, 2013
Revised: February 3, 2014
Published: February 17, 2014

ACS Publications © 2014 American Chemical Society

dx.doi.org/10.1021/jp412628y | J. Phys. Chem. A 2014, 118, 1309−1319

application of the hydrothermal method to the conversion of carbohydrate-rich biomass into value-added chemicals.

Water is required for the hydrolytic cleavage of the glycosidic bonds into monocarbohydrates, $C_6H_{12}O_6$. An interesting question is in which state water is more reactive as a reactant, in the bulk or in the solitary. The solitary water is more reactive in the glycosidic-bond cleavage in a disaccharide D-cellobiose because of the extensive breakdown of the hydrogen bonds due to the presence of the dipolar aprotic solvent.[4] Moreover, for the purpose of the high-yield production of such target chemicals as 5-hydroxymethyl-2-furaldehyde (5-HMF) and anhydrous saccharides, the DMSO−water mixture, in which the water−water hydrogen bonds are dramatically broken by the dipolar aprotic solvent, was found to be a promising binary mixture solvent. 5-HMF is a center of focus today as a biomass-derived valuable that can be converted into biofuels, fine chemicals, and polymers.[18−26] In fact, the hydrothermal dehydration (partial coking) of carbohydrates can largely enhance the combustion energy density per unit mass.[27−29] We have established that the highest 5-HMF yield is obtained in the water mole fraction range 0.20−0.30 because this region gives the optimal condition for the overall effects of the competing water-dependent factors, such as the reactivity of the water molecule as a reactant of the hydrolysis, the tautomerization of the anomeric-terminal unit from the glucose type into the fructose one, and the undesired by-paths into polymeric species via anhydrous saccharides. A question raised here is whether or not the optimization strategy for a disaccharide can be directly applicable to oligosaccharides with non-terminal carbons. Because the degradation of the larger oligomers into monomers involves the slow cleavage of non-terminal glycosidic bonds, for the larger oligomers the more attentions are needed to the weights of the pathways in competition during the glycosidic-bond cleavage. By taking advantage of the in situ ^{13}C NMR method,[1−4] we quantitatively monitor all the reactant and products as a function of the reaction time.

One of the most important features of the role of water in the DMSO−water mixture disclosed previously[4] is the high reactivity of the water at a low water content. When the water is almost isolated at the water mole fraction x_w of 0.007 as in the state of "solitary water", the cleavege of the glycosidic bond in D-cellobiose is 4−5 times faster than that in pure water. It has been known that the α-1,4-glycosidic bond is broken 3−4 times faster than the β-1,4-glycosidic bond in pure water.[2] The difference in the reaction rate in pure water may arise from the difference between the geometries of the α-1,4- and β-1,4-glycosidic bonds that determines the hydrogen-bonding configuration in the vicinity of the glycosidic bond, and accordingly, the hydrogen-bonding state of the reactant water in contact with the glycosidic bond is dependent on the glycosidic-bond geometry (α-1,4 or β-1,4 type). To further scrutinize the hydrolysis rate in relation to the state of water, it is of great interest to examine the hydrolysis kinetics as a function of the water content in the DMSO−water mixture. Here we examine whether or not the difference in the cleavage rate for α-1,4 or β-1,4 types of disaccarides can be observed also when the water content is lowered and the state of water becomses more solitary.

2. EXPERIMENTAL SECTION

A series of cyclodextrins, α-cyclodextrin (99%), β-cyclodextrin (99%), and γ-cyclodextrin (99%) were purchased from Nacalai, D-maltose monohydrate (>98%) and D-cellobiose (>98%) from Wako, and deuterated dimethyl sulfoxide (DMSO, 99.8 atom % D) and water (99.95 atom % D) from ISOTEC. These were used without further purification. The concentrations of these oligosaccharides were prepared at 1.0 mol dm^{-3} (M) in a DMSO−water mixture in terms of the monomeric D-glucose unit unless otherwise stated: α-cyclodextrin (0.167 M), β-cyclodextrin (0.143 M), γ-cyclodextrin (0.125 M), D-maltose monohydrate (0.5 M), and D-cellobiose (0.5 M). The water content is denoted in terms of the mole fraction of water, x_w. The x_w value was varied in the range 0.004−1. Here the impurity water contents in the substrates were determined by use of ^1H NMR as follows: 0.4 wt % (α-cyclodextrin), 0.7 wt % (β-cyclodextrin), 0.5 wt % (γ-cyclodextrin), 0.4 wt % (D-maltose monohydrate), and 0.4 wt % (D-cellobiose), corresponding to the x_w values of 0.003, 0.004, 0.003, 0.003, and 0.003, respectively. The solvent DMSO also contained impurity water of 0.02 wt %, corresponding to the x_w value of 0.001. The sample with the lowest x_w value included only water present originally in the substrate oligosaccharide and the solvent DMSO. D-Maltose was offered as monohydrate and the hydrate water amounts to 5 wt %, which corresponds to the x_w value of 0.05. The x_w values are denoted by the initial values at the start of the reaction; during the reaction, the water content varies with time due to the hydrolysis of the glycosidic bond and the dehydration into 5-HMF and anhydrosugars, and this increases the x_w value by 0.09 at most.

The apparatus and the experimental procedures are described elsewhere.[4] The solution prepared was loaded into a Pyrex NMR tube (SHIGEMI, 5.0 or 10.0 mm o.d.). The sample tube was flame-sealed after the tube inside was purged with argon. The reaction was monitored by the in situ ^1H and ^{13}C NMR measurements. The temperature was set to 120−180 °C in the NMR probe and controlled within ±1 °C during the course of the reaction. The temperature increment up to the target temperature from 20 °C below takes less than 1 min, which is short enough and does not affect the discussion concerning the reaction kinetics; the heat-up period at each temperature can be neglected because the reaction rate totally differs by a factor of 3−4 with a temperature difference of 20 °C. In the temperature range, the pressure of the reaction system is not very far away from the ambient, so there is no pressure effect on the reaction rates; in fact, the vapor pressure for pure DMSO (bp 189 °C) is below 0.1 MPa and that for pure water is 0.2−1.0 MPa.

3. RESULTS AND DISCUSSION

First, we describe the product distribution for the cyclodextrin and D-maltose reactions in DMSO−water mixtures by taking advantage of the high-resolution in situ NMR measurements and establish the reaction scheme. Second, we discuss the difference between the non-terminal and the anomeric-terminal glycosidic bonds in the kinetics for the hydrolytic bond breakage. We further show how the effect of water content varies with the types of glycosidic bonds. Finally, we present the optimal strategy for the production of the target compound 5-HMF by tuning the water content.

3.1. ^{13}C Spectral Analysis. Let us start with the description of how the product species can be quantitatively analyzed by using the in situ NMR method as the basis of the kinetic analysis of the glycosidic-bond cleavage rate. The ^{13}C NMR chemical shift is so sensitive to the subtle differences in the molecular structure that the carbon atomic sites in the

dx.doi.org/10.1021/jp412628y | J. Phys. Chem. A 2014, 118, 1309−1319

cyclodextrins (ring oligomers), linear oligomers with different D-glucose units, and D-glucose monomer can be distinguished from each other.

3.1.1. Ring-Opening of Cyclodextrin. One of our main purposes is to determine the cleavage rate of the non-terminal glycosidic bond by monitoring the ring-opening of the cyclodextrins and their subsequent conversions into linear oligosaccharide intermediates. The molecular structure and the in situ ^{13}C NMR spectra of β-cyclodextrin are shown in Figures 1 and 2, respectively. In Figure 2a, we show the ^{13}C spectra in

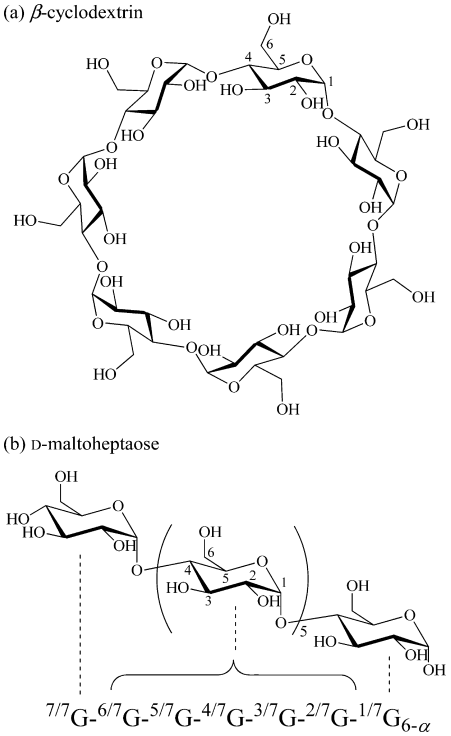

Figure 1. Notations for the D-glucose (G) units in the malto-oligosaccharides: (a) β-cyclodextrin (β-CD) and (b) D-maltoheptaose. For β-CD, seven D-glucose units are chemically and magnetically equivalent to each other, and the position of the D-glucose unit is not distinguishable. For D-maltoheptaose, the position of the D-glucose unit is denoted in the superscripts as $^{1/7}$G–$^{7/7}$G. The numbering starts from the (rightmost) anomeric-terminal unit that can be isomerized or tautomerized with the ring-opening of the D-glucose unit. The carbon atomic sites in the D-glucose unit are numbered as shown in the figure.

the chemical-shift region of the C1 carbons of saccharides; the numbering of the carbon atoms of the D-glucose unit is indicated in Figure 1. The initial spectrum in Figure 2a was taken at 0 h, i.e., immediately after the sample was heated to the reaction temperature of 140 °C. There is observed a single peak for the C1 carbon of β-cyclodextrin due to the high symmetry. The spectrum at 3 h is shown in Figure 2b. At this reaction time, 18% of β-cyclodextrin remained uncleaved and the fragmentation of D-maltoheptaose into smaller malto-oligosaccharides and D-glucose only partially proceeded; the C1 peaks for the monomer D-glucose and those for linear malto-oligosaccharides in addition to the remaining reactant of β-cyclodextrin are simultaneously observed. Here it should be noted that the C1 peaks for the non-anomeric units of the linear malto-oligosaccharides are completely separated from that for β-cyclodextrin, reflecting the subtle differences in the intramolecular moieties between the linear and ring malto-

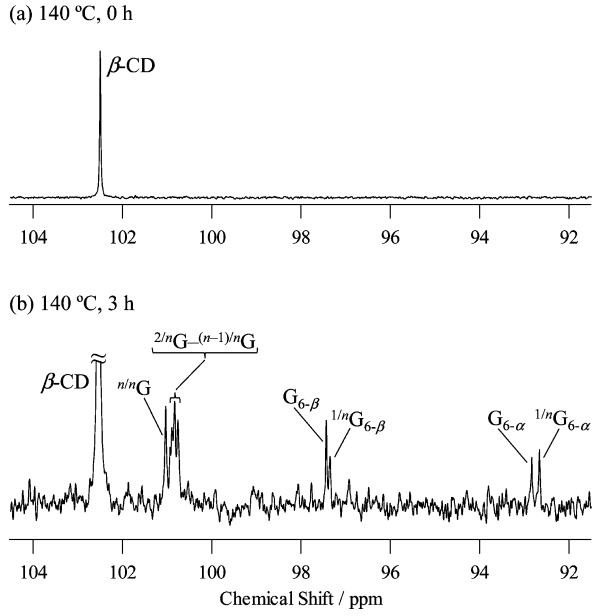

Figure 2. In situ ^{13}C spectra for β-cyclodextrin in the DMSO–water mixture at 140 °C with x_w = 0.30 at the reaction time of (a) 0 h and (b) 3 h. In panel b, the vertical axis is enlarged by a factor of 20.

oligosaccharides. This is the key advantage of the use of the cyclodextrin for the spectral and kinetic analysis. The clear distinguishability allows us to determine the cleavage rate of the non-terminal glycosidic bonds.

For a better understanding of the oligosaccharide fragmentation scheme, let us explain the notations of the D-glucose units in the malto-oligosaccharides introduced in Figure 1; the notations are common to those in ref 2. The monomer unit of D-glucose is simply expressed as G. The D-glucose unit is numbered in order from the (rightmost) anomeric terminal to the opposite non-anomeric terminal. The location of the ith unit from the anomeric terminal in the malto-oligosaccharides composed of n units is expressed as i/n in the superscript; see Figure 1b. The anomeric-terminal unit can take α- and β-types through isomerization via the ring-opening of a D-glucose unit and its isomeric form is specified by the subscript; for example, the pyranose (six-membered ring) of α-type is expressed as 6-α. In the present study, the fractions of the furanoses (five-membered ring) are below the detection limit. For the units other than the anomeric terminal, the notation of the isomeric form is omitted for brevity because the unit at any position is of the 6-α type.[2]

We indicate the positions of the D-glucose units and the glycosidic bonds also in terms. The correspondence between the terms and the numbering is given by taking the heptamer as an example as follows. For the positions of the D-glucose units, "anomeric" or "anomeric-terminal", indicates $^{1/7}$G, "non-anomeric terminal" indicates $^{7/7}$G, which is the opposite end of the anomeric terminal, and "non-terminal" indicates the internal units of $^{2/7}$G to $^{6/7}$G. The glycosidic bonds are categorized according to whether or not the bond is connected to the anomeric-terminal D-glucose unit. The bond connects the anomeric-terminal unit with the next one ($^{2/7}$G–$^{1/7}$G) and is called an "anomeric-terminal" glycosidic bond, and the other bonds, $^{7/7}$G–$^{6/7}$G to $^{3/7}$G–$^{2/7}$G, are called "non-anomeric terminal" or "internal" bonds.

3.1.2. Fragmentation of Linear Malto-oligosaccharides. After the ring-opening of β-cyclodextrin, the fragmentation of

dx.doi.org/10.1021/jp412628y | J. Phys. Chem. A 2014, 118, 1309–1319

D-maltoheptaose into smaller oligomers proceeds. Let us take a close look at the ^{13}C NMR spectra for the dimer (D-maltose) to the heptamer (D-maltoheptaose) used for the quantitative analysis of the fragmentation. Figure 3 shows the enlarged view

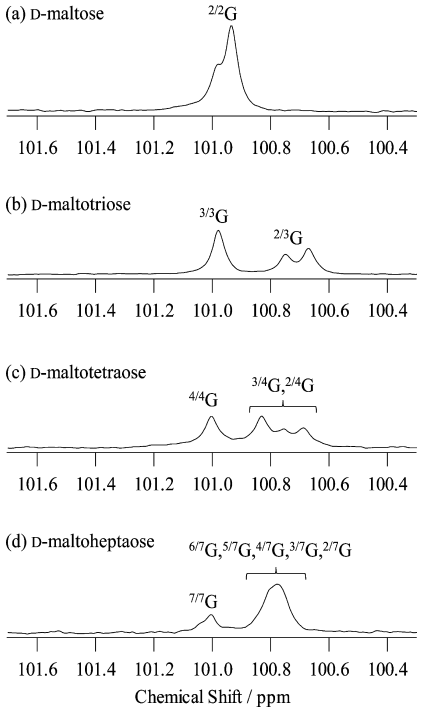

Figure 3. Enlarged view of the ^{13}C spectra for the C1 carbons of the non-anomeric terminal and the non-terminal D-glucose units for a series of malto-oligosaccharides as the authentic species: (a) D-maltose, (b) D-maltotriose, (c) D-maltotetraose, and (d) D-maltoheptaose. Spectra a, b, and c are obtained at 100 °C in pure water, taken from ref 2. Spectrum d is obtained at 80 °C in the DMSO−water mixture with x_w = 0.30. These spectral intensities are normalized so that the integral of the peaks at 100.6−101.0 ppm at each reaction time is the same. The details for the peak assignment have been described in ref 2.

of the region of the non-anomeric C1 carbon of the malto-oligosaccharides. The sharp peak at 101.0 ppm, observed in all of the dimer to the heptamer, is assigned to the C1 carbon of the non-anomeric terminal ($^{n/n}G$; n = 2−7). In the dimer spectrum in panel a, there is only one peak for the non-anomeric terminal ($^{2/2}G$), and in the trimer spectrum in panel b, there are observed two clearly separated peaks for the non-anomeric terminal ($^{3/3}G$) and the non-terminal ($^{2/3}G$). In the spectra c and d for the tetramer and the heptamer, respectively, the peaks for the non-terminal D-glucose units ($^{2/4}G$ and $^{3/4}G$ for the tetramer and $^{2/7}G$ to $^{6/7}G$ for the heptamer) are observed in the range 100.6−100.9 ppm and they are separated from the peak for the non-anomeric terminal unit ($^{4/4}G$ and $^{7/7}G$) at 101.0 ppm. Thus, for all the oligomers from dimer to heptamer, the non-anomeric terminal unit can be distinguished from the non-terminal units. The fraction of the non-anomeric terminal unit can be quantified from the relative intensity of the peak at 101.0 ppm in the entire range of C1 carbons of 100.6−101.0 ppm. Here, the fraction is denoted as θ, and θ is expressed in terms of the D-glucose unit notations introduced above as $\theta = \sum_{n=2}^{7}[^{n/n}G]/\{\sum_{n=2}^{7}(\sum_{i=2}^{n}[^{i/n}G])\}$. Because the fraction θ of the non-anomeric terminal unit increases with decreasing molecular size of the oligomers, θ can be utilized to quantitatively evaluate the time evolution of the hydrolysis fragmentation of the oligosaccharides. As can be seen from the ^{13}C spectra at different reaction times shown in Figure 4, the

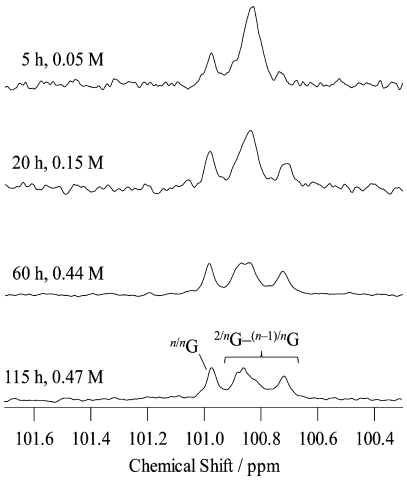

Figure 4. Time evolution of the spectrum of the C1 carbons of the non-anomeric terminal and the non-terminal during the course of the fragmentation of β-cyclodextrin into smaller oligosaccharides at 120 °C with x_w = 0.30. The spectrum at 5 h was obtained at 30 °C after quenching the reaction so that the peaks with high signal-to-noise ratio can be detected (see Figure SI-1 in the Supporting Information for the corresponding in situ spectrum at 120 °C). The initial concentration of β-cyclodextrin is 0.286 M (corresponding to 2.0 M of the monomeric D-glucose unit). The peaks at 101.0 and 100.6−100.9 ppm are respectively assigned to the non-anomeric terminal ($^{n/n}G$) and non-terminal D-glucose units ($^{2/n}G$ to $^{(n-1)/n}G$; n = 3−7) for the mixture of the dimer to the heptamer. The reaction times and the concentrations of the non-anomeric D-glucose units are indicated in the figure. The spectral intensities are normalized so that the integral of the peaks at 100.6−101.0 ppm at each reaction time is the same.

relative intensity of the non-anomeric terminal unit at 101.0 ppm increases with the reaction time; the ratio of the non-anomeric terminal peak to the non-terminal peak is 0.16, 0.20, 0.25, and 0.32, respectively, at 5, 20, 60, and 115 h, respectively. The time evolution of the fraction θ will be further discussed on the basis of the rate equations in section 3.2.2.

3.2. Glycosidic-Bond Cleavage. *3.2.1. Cleavage Rates of Non-Terminal Glycosidic Bonds of Cyclodextrins.* In Figure 5a,b, we show the time evolutions of the concentrations of the reactant and products of the β-cyclodextrin reactions at 120 and 180 °C, respectively, with x_w = 0.30. At the water content of x_w = 0.30, the 5-HMF production yield from D-cellobiose has been optimized;[4] the effect of the water content will be discussed in section 3.3.2. The lower temperature of 120 °C was employed to obtain the time evolution with high time resolution with the sufficient number of NMR signal acquisitions. The progress of the reaction in Figure 5a corresponds to that in the early time region up to ∼2 h at the higher temperature of 180 °C in Figure 5b. As seen in Figure 5a, the amount of β-cyclodextrin decreases monotonically due to the ring-opening caused by the glycosidic-bond cleavage. It is noteworthy that D-glucose is observed in nearly an equal molar quantity to the linear malto-oligosaccharides. The early ratio of 1:1 corresponds to the D-glucose and the residual oligomeric fragments. The simple ratio is maintained up to ∼60 h at 120 °C (Figure 5a) because the glycosidic-bond cleavage of the anomeric-terminal unit is by far faster compared to the non-terminal and non-anomeric terminal ones due to the tautomerization of the glucose-type

dx.doi.org/10.1021/jp412628y | J. Phys. Chem. A 2014, 118, 1309−1319

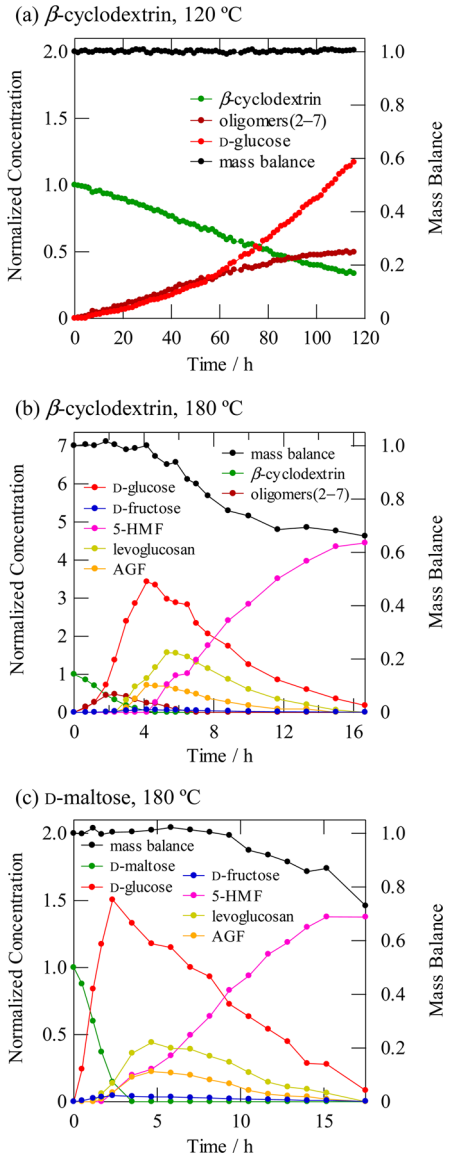

Figure 5. (a, b) Time evolutions of the concentrations of the reactant and products for the reactions of β-cyclodextrin at 120 and 180 °C, respectively, with $x_w = 0.30$. (c) Time evolutions of the concentrations of the reactant and products for the reaction of D-maltose at 180 °C with $x_w = 0.30$. The vertical axis on the left shows the normalized concentration, and that on the right shows the mass balance. The normalized concentration denotes the concentration of the compound of interest divided by the initial substrate concentration. The mass balance denotes the ratio of the sum of the amount of carbon atoms in the reactant and the products detected by ^{13}C NMR at each reaction time divided by the carbon amount in the reactant in the beginning of the reaction.

anomeric-terminal unit into the more easily cleavable fructose-type one.[2,4]

There exists a large difference in the cleavage rate between a non-terminal glycosidic bond and an anomeric-terminal one. This is clearly seen in the comparison of the hydrolysis rate of β-cyclodextrin with that of D-maltose in Figure 5c. The decrease in the concentrations of β-cyclodextrin (*seven* non-terminal bonds) and D-maltose (*one* anomeric-terminal bond) occurs on a similar time scale. This means that the cleavage of the anomeric-terminal glycosidic bond in D-maltose is faster than that in β-cyclodextrin. Here it is important to note that the ring-opening of β-cyclodextrin occurs when any of the *seven* glycosidic bonds is cleaved. In other words, the hydrolysis cleavage rate of a single glycosidic bond in β-cyclodextrin is 1/7 of the decreasing rate of the β-cyclodextrin concentration when we make a comparison with that in D-maltose. This is expressed in terms of the rate equations for the decomposition of the cyclodextrins and D-maltose as follows:

$$\frac{d[\xi\text{-CD}]}{dt} = -nk_{\xi\text{-CD}}[\xi\text{-CD}] \quad (1)$$

$$\frac{d[\{\text{D-maltose}\}]}{dt} = -k_{mal}[\{\text{D-maltose}\}] \quad (2)$$

where $k_{\xi\text{-CD}}$ and k_{mal} are the first-order rate constants for a cyclodextrin (CD) and D-maltose, n is the number of the D-glucose units in the cyclodextrin, which is 6, 7, and 8 when ξ is α, β, and γ, respectively, t is the reaction time, and the square brackets express the concentration. The curly brackets in eq 2 indicate that all the possible isomers are treated collectively because the mutual isomerizations of D-maltose are rapid enough to be treated collectively in the pre-equilibrium states as confirmed for other sugars in the previous studies.[1−4] By this definition, the effect of the water concentration is implicitly included in the rate constants. The rate constants are determined by using the data within the time region where neither the acidic byproducts nor the mass-balance loss due to the polymerization need to be taken into account, typically up to 2−12 h, depending on the reaction temperature and the water content.

The rate constants, $k_{\beta\text{-CD}}$ and k_{mal}, were determined at the water mole fraction of $x_w = 0.30$ in the temperature range 120−180 °C, as summarized in Table 1. The values of k_{mal} are larger

Table 1. Rate Constants for Hydrolytic Glycosidic-Bond Cleavage of β-Cyclodextrin ($k_{\beta\text{-CD}}$) and D-Maltose (k_{mal}) in a DMSO−Water Mixture with $x_w = 0.30$ at Temperatures of 120−180 °C

T/°C	$k_{\beta\text{-CD}}/s^{-1}$	k_{mal}/s^{-1}
120	$(5.8 \pm 0.2) \times 10^{-7}$	$(6.0 \pm 0.2) \times 10^{-6}$
130	$(1.2 \pm 0.1) \times 10^{-7}$	$(1.1 \pm 0.1) \times 10^{-6}$
140	$(4.4 \pm 0.5) \times 10^{-6}$	$(4.1 \pm 0.3) \times 10^{-5}$
150	$(7.0 \pm 0.4) \times 10^{-6}$	$(5.1 \pm 0.7) \times 10^{-5}$
180	$(2.5 \pm 0.3) \times 10^{-5}$	$(1.5 \pm 0.3) \times 10^{-4}$

by a factor of 6−10 than those of $k_{\beta\text{-CD}}$ over the temperature range examined. The cleavage of the anomeric-terminal glycosidic bond in D-maltose proceeds more rapidly than that of the non-terminal one in β-cyclodextrin. This is in harmony with the previous kinetic results for the hydrothermal decompositions of the linear malto- and cello-oligosaccharides into the monomers via the keto−enol tautomerization of the anomeric-terminal D-glucose unit into the D-fructose one.[2]

To see the effect of the ring size on the glycosidic-bond cleavage rate, we made a comparison of the reactions of α-, β-, and γ-cyclodextrins (six-, seven-, and eight-membered, respectively) at 180 °C with $x_w = 0.30$; the time evolutions are given in Figure SI-2 in the Supporting Information. The ring-size dependence was found to be rather weak. The determined rate constants per glycosidic bond for α-, β-, and γ-cyclodextrins are $(2.9 \pm 0.4) \times 10^{-5}$, $(2.5 \pm 0.3) \times 10^{-5}$, and $(2.1 \pm 0.3) \times 10^{-5}$ s^{-1}, respectively. A relatively small effect of the ring size can be understood to be due to the ring strain,

dx.doi.org/10.1021/jp412628y | J. Phys. Chem. A 2014, 118, 1309−1319

which is larger for the smaller cyclodextrin. More importantly, the difference between the non-terminal and the anomeric-terminal glycosidic bonds is 1 order of magnitude larger than the effect caused by the ring strain. The tautomerization at the anomeric-terminal unit plays the essential role in controlling the glycosidic-bond cleavage.

3.2.2. Cleavage Rates of Non-Terminal Glycosidic Bonds in Linear Malto-Oligosaccharides. Let us move on to the kinetics of the hydrolytic fragmentation of the linear D-maltoheptaose generated from β-cyclodextrin by the ring-opening. The degree of the fragmentation can be evaluated by the quantity of the fraction of the terminal unit in the total units other than the anomeric-terminal one; in terms of the notations introduced in section 3.1.1, the fraction is equal to the ratio of the non-anomeric terminal D-glucose ($^{n/n}$G) to the non-anomeric D-glucose units ($^{2/n}$G to $^{n/n}$G; n = 2−7). This quantity can be experimentally determined from the ^{13}C NMR spectrum for the C1 carbon of the non-anomeric units in terms of the fraction $\theta = \sum_{n=2}^{7}[^{n/n}\mathrm{G}]/\{\sum_{n=2}^{7}(\sum_{i=2}^{n}[^{i/n}\mathrm{G}])\}$ introduced in section 3.1.2. The quantity θ measures the extent of the fragmentation into smaller oligomers. The θ values thus calculated (θ_{cal}) for the dimer to the heptamer are in the range 0.17−1. The θ values independently observed by ^{13}C NMR (θ_{obs}) for the authentic samples of pure dimer to heptamer are in good agreement with θ_{cal}, as shown in Figure 6.

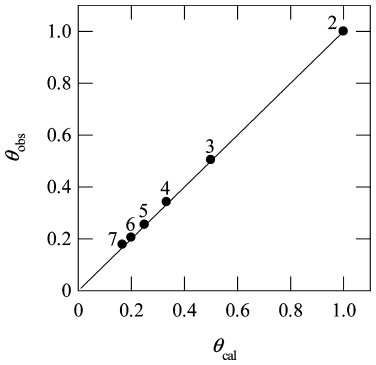

Figure 6. Plots of the θ value observed by NMR (θ_{obs}) against the calculated one (θ_{cal}). The θ_{obs} value was determined by the ^{13}C NMR integral intensities of the signals of the non-anomeric terminal and internal D-glucose units. The θ_{cal} value was calculated using eq 16 in the Appendix for each pure malto-oligosaccharide. The number for each plot in the figure is that of the D-glucose units in the oligosaccharide and the solid line represents $\theta_{obs} = \theta_{cal}$.

This verifies the quantitative validity of the present analysis for the fragmentation kinetics of linear oligosaccharides described below. In Figure 7, the fraction θ for the decomposition of β-cyclodextrin examined at 120 °C with x_w = 0.30 is plotted against the reaction time. The θ value monotonically increases with the time from 0.17 in the beginning, and it finally reaches 0.33 after 115 h, at which 67% of β-cyclodextrin is decomposed.

Let us discuss the cleavage rates of the internal and anomeric-terminal glycosidic bonds that determine the time evolution of the fraction θ. Here we briefly summarize the procedure to determine the cleavage rate constant for the non-anomeric glycosidic bonds; the details are described in the Appendix. The curve fitting of θ was carried out with only a single variable parameter of the cleavage rate constant $k_{non\text{-}at}$ for the non-anomeric glycosidic bond. In the fitting of θ in Figure 7, the cleavage rate constants $k_{1/n}$ for the anomeric terminal and

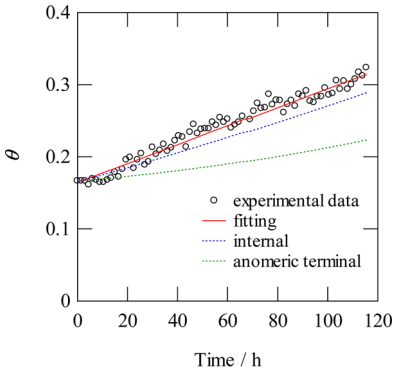

Figure 7. Time dependence of the fraction θ of the non-anomeric terminal D-glucose ($^{n/n}$G) among the non-anomeric D-glucose units ($^{2/n}$G to $^{(n-1)/n}$G; n = 2−7) for the mixture of the dimer to the heptamer during the course of the decomposition of β-cyclodextrin into smaller oligomers. The open symbols are the experimental results, and the solid curve is the fitting result. The broken curve denoted as internal (blue) is the plot of the θ value estimated with k_{at} = 0 representing the contribution of the internal bond cleavage, and that denoted as anomeric terminal (green) is the result with $k_{non\text{-}at}$ = 0 representing the contribution of the anomeric-terminal bond cleavage.

$k_{\beta\text{-CD}}$ for β-cyclodextrin are treated as the fixed parameter. For the $k_{1/n}$ value from the trimer to the heptamer, we employed the rate constant for D-maltose, k_{mal} ($=k_{1/2}$). The rate constants k_{mal} and $k_{\beta\text{-CD}}$ were determined independently in the reactions of D-maltose and β-cyclodextrin, respectively, as the starting materials. The $k_{non\text{-}at}$ value was determined by numerically integrating the simultaneous rate equations for all the oligomers to obtain the time evolution of the fraction θ in Figure 7, where the mass balance is kept constant over the reaction time, as shown in Figure 5a. These formulations are completely satisfactory for the present purpose to discuss the relative rates of the cleavage of the internal and anomeric-terminal glycosidic bonds; the validations based on experimental results are described in the Appendix.

The $k_{non\text{-}at}$ value thus determined at 120 °C is (6.4 ± 0.2) × 10^{-7} s^{-1}. This value of $k_{non\text{-}at}$ is close to that of $k_{\beta\text{-CD}}$ of (5.8 ± 0.2) × 10^{-7} s^{-1} at 120 °C and is 1 order of magnitude smaller than that of k_{mal}, (6.0 ± 0.2) × 10^{-6} s^{-1}. This indicates that the kinetics for the cleavage of the non-terminal glycosidic bond in the linear oligomers is similar to that in the cyclodextrins, which supports our kinetic insights that the anomeric-terminal glycosidic bond is broken more rapidly than the non-anomeric one. It is to be noted, on the other hand, that the slower internal-bond cleavage is of significance for the fragmentation of D-maltoheptaose. In Figure 7, the contributions of $k_{non\text{-}at}$ and k_{at} to the change in θ are shown as the broken curves; the contribution of $k_{non\text{-}at}$ (denoted as internal in Figure 7) was evaluated by setting k_{at} to 0 with $k_{non\text{-}at}$ kept at the value of the fitting result as determined above, and the contribution of k_{at} (denoted as anomeric terminal) evaluated vice versa. In the earlier time region, the time evolution of θ is mainly determined by the contribution of $k_{non\text{-}at}$. This can be of more significance for larger polysaccharides like starch and cellulose.

On the basis of the time evolution analysis, the reaction scheme for the hydrolytic decomposition of β-cyclodextrin can be summarized as in Figure 8. First, β-cyclodextrin is hydrolyzed into D-maltoheptaose through the non-terminal glycosidic-bond cleavage. Subsequently, the anomeric-terminal

dx.doi.org/10.1021/jp412628y | J. Phys. Chem. A 2014, 118, 1309−1319

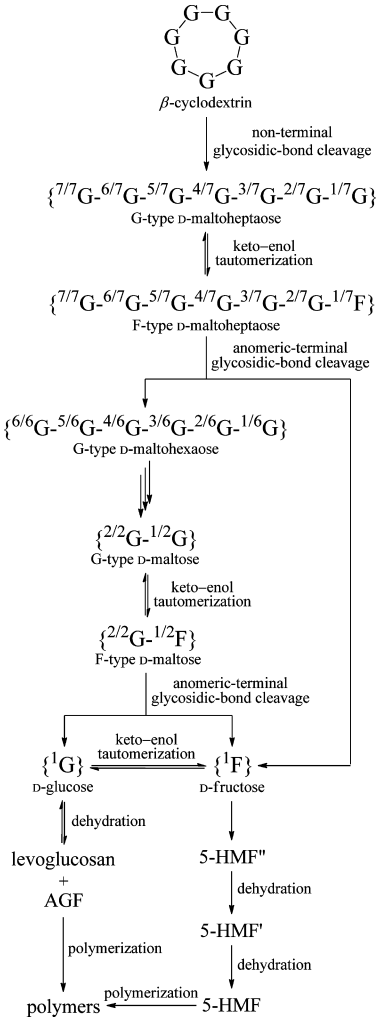

Figure 8. Non-catalytic conversion scheme from β-cyclodextrin in the DMSO–water mixture into 5-HMF. The curly brackets denote a set of all isomers (pyranoses and furanoses of α- and β-types and open-chain form) of each saccharide. The unit F stands for the monomer unit of D-fructose. Three arrows represent the repeat of the hydrolytic cleavage at the anomeric-terminal glycosidic bond after the keto–enol tautomerization from the original glucose-type oligomer into the fructose-type one.

D-glucose unit is selectively eliminated from the malto-oligosaccharides after the tautomerization into the D-fructose one. The cleavage of the internal bonds proceeds in parallel with the cleavage of the anomeric-terminal bond, with the reaction rate per bond 1 order of magnitude slower than that of the anomeric-terminal one. Though slower, the internal-bond cleavage plays an important role in particular in the early time region because of the presence of the larger number of the internal bonds than the anomeric-terminal ones; the logic is the same as that for the similar decomposition rates observed for D-maltose and β-cyclodextrin. The number of anomeric-terminal D-glucose units increases with the fragmentation via the internal-bond cleavage, and thus the contribution of the faster anomeric-bond cleavage becomes more dominant as the reaction proceeds.

The reaction steps following the monomerization into D-glucose, corresponding to the time region after ~3 h in Figure 5b, can be understood essentially in terms of the scheme and pathways that have been established for D-cellobiose as discussed elsewhere.[4] In these steps, D-glucose is reversibly transformed into D-fructose via keto–enol tautomerization and D-fructose is dehydrated into 5-HMF through the precursors of 5-HMF″ (with no double bond) and 5-HMF′ (with one double bond).[3] There are also reversible by-paths into the anhydromonosaccharides of 1,6-anhydro-β-D-glucopyranose (levoglucosan) and 1,6-anhydro-β-D-glucofuranose (AGF). The polymerization of these monosaccharide derivatives into NMR-undetectable solid-state species competes with the 5-HMF production. The quantitative analysis of the yields and rates of the valuable monosaccharide derivatives are described in section 3.3.

3.2.3. Effect of Water on Cleavage of Non-Terminal and Anomeric-Terminal Glycosidic Bonds. Panels a and b of Figure 9 show respectively the rate constants for the hydrolytic cleavage of the non-terminal glycosidic bonds in β-cyclodextrin ($k_{\beta\text{-CD}}$) and that of the anomeric-terminal glycosidic bond in D-maltose (k_{mal}) as a function of x_w; in panel b, the data for β-1,4-linked D-cellobiose (k_{cel}) taken from ref 4 are shown for comparison. As seen in Figure 9a, the cleavage of the non-terminal glycosidic bond in β-cyclodextrin gets much faster with decreasing water content. The large reaction rate at the lower water contents is common to the case of D-cellobiose, as shown in Figure 9b. Such enhancement of the cleavage rate is due to the high reactivity of the "solitary water". The solitary

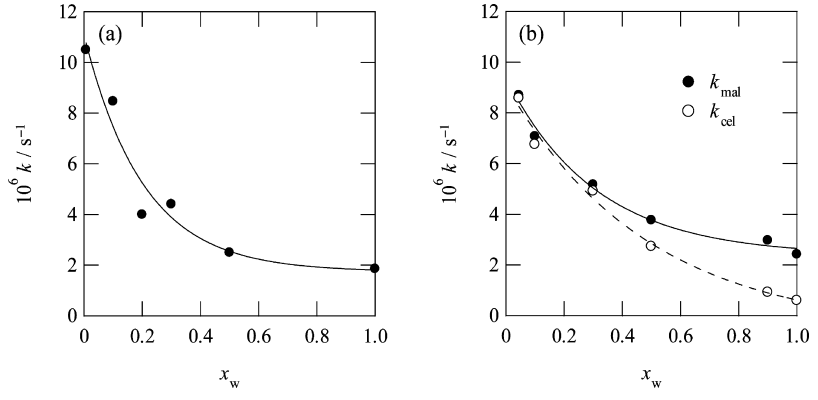

Figure 9. (a) Rate constant for the cleavage of the glycosidic bond in β-cyclodextrin ($k_{\beta\text{-CD}}$) at 140 °C plotted against x_w. (b) Rate constants for the cleavage of the glycosidic bonds in D-maltose (k_{mal}) and D-cellobiose (k_{cel}) at 120 °C plotted against x_w. The solid and dashed curves are guides for eyes.

dx.doi.org/10.1021/jp412628y | J. Phys. Chem. A 2014, 118, 1309–1319

water is in the state of water in which the water is isolated from other water molecules and its partial charges are more naked because of the absence of the hydrogen bonding to water molecules nearby.[5−7] In the low x_w region below ∼0.05, the contact probability between water molecules is negligibly small, as evaluated on the basis of the simple estimation of the coordination number.[4]

3.2.4. Comparison of Water-Content Dependencies between α- and β-1,4-Glycosidic Bonds. Here we discuss the difference in the water-content dependence of the glycosidic-bond breakage between the α- and β-1,4-linked disaccharides; the former and the latter have, respectively, the glycosidic-bond geometry involved in starch and cellulose. As seen in Figure 9b, the variation of the k_{cel} values for D-cellobiose with x_w is larger than that of the k_{mal} values for D-maltose. The difference in the water-content dependence can be ascribed to the differences in the bond orientation and in the bond length of the C1−O−C4 moiety between the α- and β-1,4-glycosidic bonds. These structural factors can affect the contact probability and hydration dynamics of the reactant water. The α-1,4-glycosidic bond is in the axial direction against the plane of the sugar ring (hydrophobic), whereas the β-1,4-glycosidic bond is in the equatorial. The β-1,4-glycosidic bond length calculated by using ab initio MO method is shorter by ∼0.04 Å than that of the α-1,4-glycosidic bond.[2] On the basis of the sugar-ring orientation and the bond length, we suggest that the hydrophobic moiety (or the sugar ring) of the β-1,4-linked D-cellobiose can be located closer to the glycosidic bond than that of the α-1,4-linked D-maltose. The sugar ring provides a more or less hydrophobic moiety for the water molecule approaching the glycosidic bond as a reactant of the hydrolysis. In pure water (x_w = 1), the population of water molecules in the C1−O−C4 moiety of D-cellobiose might be more or less smaller than that in D-maltose. This can be one of the reasons for the slower hydrolytic breakage of glycosidic bond at higher water contents. The solitary water existing at the lower water contents, on the other hand, can be distributed more preferentially in the vicinity of the C1−O−C4 moiety, regardless of the type of glycosidic bond, α-1,4 or β-1,4 type. In this situation, there is absent the competing hydrogen bonds that can disturb the attractive interactions between the solitary water and the glycosidic-bond oxygen. In other words, the high reactivity of the solitary water overwhelms the effect of the glycosidic-bond geometry on the cleavage rate. At lower water contents, the glycosidic-bond cleavage of D-cellobiose is therefore markedly enhanced and its rate becomes almost the same as that for D-maltose.

Let us then see the water-content effect on the tautomerization of the anomeric D-glucose residue in the α-1,4-linked disaccharide, D-maltose, into the D-fructose one. As illustrated in Figure 10, the higher the water content, the larger the D-fructose/D-glucose (F/G) ratio. At the high water contents of x_w = 0.90−1, the F/G ratio in the beginning of the reaction is over the equilibrium value of 0.11 in pure water at 120 °C,[1] and it decreases with the reaction time and finally approaches the equilibrium. The large F/G ratio arises from the glycosidic-bond breakage after the formation of the reactive intermediate of the fructose-type D-maltose, whose anomeric D-glucose residue is transformed into the D-fructose one. At the low water contents of x_w = 0.05−0.50, in contrast, the F/G ratio is as low as 0.02−0.05. In this case, the F/G ratio attains equilibrium within 1 h. The small F/G ratio at x_w = 0.05−0.50 is due to the competing reaction steps, such as the back-

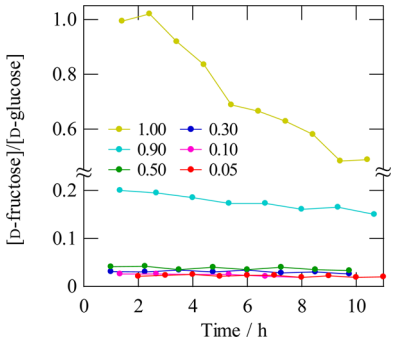

Figure 10. Water-content dependence of the population ratio, [D-fructose]/[D-glucose], in the reaction of D-maltose examined at 120 °C. The x_w values are indicated in the figure. The data in pure water (x_w = 1) are taken from ref 2.

transformation of D-fructose into D-glucose and the successive consumption of D-fructose through the conversion into 5-HMF, which are much faster in DMSO than in water.[4] The difference of the F/G ratio for D-maltose on the water content x_w is almost exactly the same as that for D-cellobiose, as shown in Figure SI-3 in the Supporting Information. This means that the tautomerization kinetics and equilibrium of the anomeric unit between the glucose type and the fructose type is essentially independent of the geometries of the anomeric-terminal glycosidic bond.

3.2.5. Temperature Effect. The Arrhenius plots for the rate constants $k_{β\text{-CD}}$ and k_{mal}, defined respectively by eqs 1 and 2, are shown in Figure 11. The E_a value (94 ± 5 kJ mol^{-1}) for the

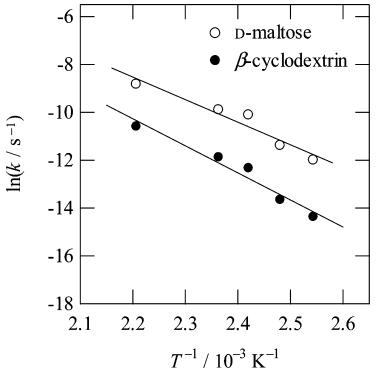

Figure 11. Arrhenius plots of the rate constants for the cleavage of the glycosidic bonds in β-cyclodextrin ($k_{β\text{-CD}}$, ●) and D-maltose (k_{mal}, ○) at x_w = 0.30. The activation energies for β-cyclodextrin and D-maltose are 94 ± 5 and 78 ± 6 kJ mol^{-1}, respectively.

non-terminal glycosidic-bond breakage of β-cyclodextrin is larger by 16 kJ mol^{-1} compared with that (78 ± 6 kJ mol^{-1}) for the anomeric-terminal glycosidic-bond breakage of D-maltose. This is in harmony with the conclusion stated above that the transformation of the anomeric-terminal D-glucose unit into the D-fructose significantly lowers the reaction barrier of the glycosidic-bond cleavage. Furthermore, the E_a value for D-maltose linked by α-1,4-glycosidic bond is smaller by 11 kJ mol^{-1} when compared to that (89 ± 4 kJ mol^{-1}) for D-cellobiose linked by β-1,4-glycosidic bond. This is in parallel to the observation that the rate for the hydrolysis of D-maltose is faster than that of D-cellobiose.

3.3. Dehydration of D-Glucose and D-Fructose. *3.3.1. Monosaccharide Derivatives.* Subsequently to the

dx.doi.org/10.1021/jp412628y | J. Phys. Chem. A 2014, 118, 1309−1319

glycosidic-bond cleavage of β-cyclodextrin and D-maltose, as seen in the time evolutions shown in Figure 5b,c, respectively, D-glucose generated is transformed into D-fructose and successively into 5-HMF via the precursor with no double bond (5-HMF″) and that with one double bond (5-HMF′) as in the case of D-fructose transformation into 5-HMF in pure DMSO.[3] After ∼2 h, the anhydromonosaccharides of levoglucosan and AGF are generated through other dehydration path from D-glucose. These anhydrosugars are reversibly hydrated into D-glucose or polymerized into NMR-undetectable species. When the water content is changed, the product species are common and only their populations are varied. At the lower water contents, the anhydromonosaccharides of levoglucosan and AGF are produced more, and the production of the precursors of 5-HMF″ and 5-HMF′ becomes more favorable. These observations are common to those for D-cellobiose in the DMSO−water mixture.[4] For 5-HMF, the yield is also dependent on the water content, as described in detail in the following section.

3.3.2. Water-Content Dependence of 5-HMF Yield. So far, much attention has been paid to the generation of 5-HMF (5-hydroxymethyl-2-furaldehyde) from biomass-derived carbohydrates.[20−26] This is because 5-HMF is regarded as a potential platform chemical with a wide application profile.[18,19] Once we succeed in obtaining the reactive monomer from such biomass as starch (edible) and cellulose (inedible), this can meet the increasing demand for green and sustainable chemistry. In many studies, rare earth metals and acids were used as catalysts, and the 5-HMF yields from starch and cellulose achieved by using such non-green methods are at most 53% and 48%, respectively.[20] It is to be noted that even when a simple monosaccharide, D-glucose, was used as the reactant, the yield of 76−80% was achieved.[20] Recently, we have found that the yield of 5-HMF produced from the disaccharide D-cellobiose can be controlled by tuning the water content in DMSO−water mixtures and that the yield can be maximized up to ∼70% at the low water content of x_w = 0.20−0.30.[4] Here we focus on the 5-HMF yield from the higher-oligomeric cyclodextrins. As shown in Figures 5 and SI-2 in the Supporting Information, the time dependence of the 5-HMF yield reaches a maximum. The reaction time longer than the maximum time of the yield of 5-HMF leads to the yield loss into the undesired polymerization path as revealed previously.[4] For the purpose of determining the optimal water content, we have examined the maximum yield as a function of the x_w value. In Figure 12, the maximum yield in the reaction of β-cyclodextrin at 180 °C is plotted against x_w. The highest yield of 64% is attained with x_w = 0.30 (at 16 h). This yield is essentially the same as the maximum yield of 66% obtained from the disaccharide D-cellobiose with x_w = 0.30 at the same temperature.[4] The yield of 64% is significantly higher than that of 46% obtained from D-glucose in hot pure water.[4] The loss of the 5-HMF yield at higher water contents comes mainly from the polymerization enhanced by water. At the lower water contents, the polymerization of the anhydromonosaccharides of levoglucosan and AGF lowers the 5-HMF yield. These polymerization paths were found to be enhanced by a temperature increase in the previous study on the D-cellobiose decomposition in the DMSO−water mixture.[4] A higher maximum yield of 5-HMF could be attained by taking a lower reaction temperature if the longer reaction time required accordingly would be acceptable. The maximum yields of 5-HMF are almost the same in the reactions of the cyclodextrins and D-maltose. In other words, the maximum yield is almost independent of the degree of oligomerization up to the heptamer. When 5-HMF is produced by starting from D-fructose, the yield is as high as 95% with much less yield loss into undesirable polymerization by-paths shown in Figure 8. The glycosidic-bond cleavages of D-cellobiose and D-maltose are not the rate-determining step of the 5-HMF production because the time scale is sufficiently smaller than that of the conversion from D-glucose to 5-HMF. Thus the conversion of D-glucose into D-fructose is considered to be the rate-determining step. In the case of the biomass utilization, it is to be noted that the situation can be dramatically changed by the slow rate of the cleavage of the non-terminal glycosidic bonds.

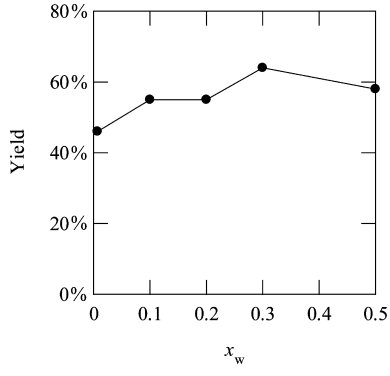

Figure 12. Maximum yield of 5-HMF in the reaction of β-cyclodextrin at 180 °C plotted against x_w.

4. CONCLUSIONS

We have investigated the conversions of α-, β-, and γ-cyclodextrins with the non-terminal glycosidic bond and D-maltose with the anomeric-terminal one into valuable 5-HMF in the DMSO−water mixture. By taking advantage of the in situ ^{13}C NMR spectroscopy to determine the product time evolution with the mass balance confirmed, we have quantitatively evaluated the difference in the cleavage kinetics between the non-terminal and the anomeric-terminal glycosidic bonds and showed how to control the pathways and kinetics by tuning the water content. The cleavage rate constants for the non-terminal glycosidic bonds of both cyclodextrins and linear malto-oligosaccharides have been found to be significantly small compared to that for the anomeric-terminal glycosidic bond because the tautomerization of the D-glucose unit into the more reactive, easily cleavable D-fructose unit is impossible for the monomer units in the cyclodextrins. The glycosidic-bond cleavage is faster at the lower water content, because of the high reactivity of solitary water molecules with the large partial charges more naked. The dependency on the water content is larger for the β-1,4-glycosidic bond in D-cellobiose than for the α-1,4-glycosidic bond in D-maltose. Such a difference arising from the type of glycosidic bond (α or β) can be interpreted as the hydration states of water controlled by the atomic-site geometries of bond orientation and bond length of the C1−O−C4 moiety. The 5-HMF yield of 64% obtained from β-cyclodextrin was as high as those of the disaccharides, D-maltose and D-cellobiose. The highest 5-HMF yield for both β-cyclodextrin and D-maltose was achieved at the relatively poor water content of x_w = 0.30 as in the case of D-cellobiose, at which the polymerization by-paths via 5-HMF and anhydro-monosaccharide were effectively suppressed. The optimal

dx.doi.org/10.1021/jp412628y | J. Phys. Chem. A 2014, 118, 1309−1319

condition was achieved at a moderate temperature of 180 °C without using any catalysts. This study provides a promising answer to design the biomass conversion process to develop the green chemistry.

APPENDIX

Determination of Cleavage Rate Constants for Non-Anomeric Glycosidic Bonds in Linear Malto-Oligosaccharides

The first-order rate equations for the decomposition of the malto-oligosaccharides of the dimer D-maltose (G_2) to the heptamer D-maltoheptaose (G_7) are expressed as

$$\frac{d[\beta\text{-CD}]}{dt} = -7k_{\beta\text{-CD}}[\beta\text{-CD}] \quad (3)$$

$$\frac{d[G_7]}{dt} = 7k_{\beta\text{-CD}}[\beta\text{-CD}] - (k_{6/7} + k_{5/7} + k_{4/7} + k_{3/7} + k_{2/7} + k_{1/7})[G_7] \quad (4)$$

$$\frac{d[G_6]}{dt} = (k_{6/7} + k_{1/7})[G_7] - (k_{5/6} + k_{4/6} + k_{3/6} + k_{2/6} + k_{1/6})[G_6] \quad (5)$$

$$\frac{d[G_5]}{dt} = (k_{5/7} + k_{2/7})[G_7] + (k_{5/6} + k_{1/6})[G_6] - (k_{4/5} + k_{3/5} + k_{2/5} + k_{1/5})[G_5] \quad (6)$$

$$\frac{d[G_4]}{dt} = (k_{4/7} + k_{3/7})[G_7] + (k_{4/6} + k_{2/6})[G_6] + (k_{4/5} + k_{1/5})[G_5] - (k_{3/4} + k_{2/4} + k_{1/4})[G_4] \quad (7)$$

$$\frac{d[G_3]}{dt} = (k_{4/7} + k_{3/7})[G_7] + 2k_{3/6}[G_6] + (k_{3/5} + k_{2/5})[G_5] + (k_{3/4} + k_{1/4})[G_4] - (k_{2/3} + k_{1/3})[G_3] \quad (8)$$

$$\frac{d[G_2]}{dt} = (k_{5/7} + k_{2/7})[G_7] + (k_{4/6} + k_{2/6})[G_6] + (k_{3/5} + k_{2/5})[G_5] + 2k_{2/4}[G_4] + (k_{2/3} + k_{1/3})[G_3] - k_{1/2}[G_2] \quad (9)$$

where $k_{i/n}$ is the rate constant for the cleavage of the glycosidic-bond at the ith unit from the anomeric-terminal one (i.e., the bond between $^{(i+1)/n}$G and $^{i/n}$G) in the linear oligomers composed of n units. For the reliable curve fitting for the time evolution of the fraction θ in Figure 7 to obtain the physically reasonable rate constants, in our approach we minimized the number of variable parameters as below. First, the cleavage rate constants $k_{1/n}$ (n = 2−7) for the anomeric terminal, that is, the glycosidic bond between the anomeric-terminal unit and the next one (bond between $^{1/n}$G and $^{2/n}$G), are treated to be independent of the oligomer size and are denoted collectively as k_{at}. The effect of the oligomer size on the cleavage rate of the anomeric-terminal unit has been examined for D-maltose, D-maltotriose, and D-maltotetraose, and the differences among these oligomers are only 5−10%.[2] Then, the cleavage rates for all the other internal, non-anomeric terminal glycosidic bonds are treated to be independent of the oligomer sizes and the positions and are collectively denoted as $k_{non\text{-}at}$. Although the sugar-chain flexibilities for different oligomer sizes could more or less affect the cleavage rate of the internal glycosidic bond, the magnitude of such effects should be at most 10−20% as in the case of the effect of the ring strain of different sizes of cyclodextrins, as described in section 3.2.1. On the basis of these assumptions, eqs 4−9 are rewritten as follows:

$$\frac{d[G_7]}{dt} = 7k_{\beta\text{-CD}}[\beta\text{-CD}] - (5k_{non\text{-}at} + k_{at})[G_7] \quad (10)$$

$$\frac{d[G_6]}{dt} = (k_{non\text{-}at} + k_{at})[G_7] - (4k_{non\text{-}at} + k_{at})[G_6] \quad (11)$$

$$\frac{d[G_5]}{dt} = 2k_{non\text{-}at}[G_7] + (k_{non\text{-}at} + k_{at})[G_6] - (3k_{non\text{-}at} + k_{at})[G_5] \quad (12)$$

$$\frac{d[G_4]}{dt} = 2k_{non\text{-}at}[G_7] + 2k_{non\text{-}at}[G_6] + (k_{non\text{-}at} + k_{at})[G_5] - (2k_{non\text{-}at} + k_{at})[G_4] \quad (13)$$

$$\frac{d[G_3]}{dt} = 2k_{non\text{-}at}[G_7] + 2k_{non\text{-}at}[G_6] + 2k_{non\text{-}at}[G_5] + (k_{non\text{-}at} + k_{at})[G_4] - (k_{non\text{-}at} + k_{at})[G_3] \quad (14)$$

$$\frac{d[G_2]}{dt} = 2k_{non\text{-}at}[G_7] + 2k_{non\text{-}at}[G_6] + 2k_{non\text{-}at}[G_5] + 2k_{non\text{-}at}[G_4] + (k_{non\text{-}at} + k_{at})[G_3] - k_{at}[G_2] \quad (15)$$

Here the cleavage rate constant for D-maltose, k_{mal}, is substituted into k_{at}. The rate constants, k_{mal} and $k_{\beta\text{-CD}}$, are determined independently in the reactions of β-cyclodextrin and D-maltose, respectively, as the starting material as shown in Figure 5b,c. When the integration of these differential equations is carried out, k_{mal} and $k_{\beta\text{-CD}}$ are treated as the fixed parameter with only a single variable parameter of the cleavage rate constant, $k_{non\text{-}at}$, for the non-anomeric glycosidic bond. The $k_{non\text{-}at}$ value is thus determined by numerically integrating the simultaneous rate equations to fit the time evolution of the fraction θ in Figure 7.

Once the concentrations of the dimer to the heptamer are obtained as a function of the reaction time, the fraction θ of the non-anomeric terminal units among the non-anomeric ones is obtained as

$$\theta = \frac{\sum_{n=2}^{7}[G_n]}{\sum_{n=2}^{7}(n-1)[G_n]} = \frac{[G_7] + [G_6] + [G_5] + [G_4] + [G_3] + [G_2]}{6[G_7] + 5[G_6] + 4[G_5] + 3[G_4] + 2[G_3] + [G_2]} \quad (16)$$

and this expression is used for the optimization of the variable parameter $k_{non\text{-}at}$ in the curve fitting for θ discussed in section 3.2.1.

dx.doi.org/10.1021/jp412628y | J. Phys. Chem. A 2014, 118, 1309−1319

■ ASSOCIATED CONTENT

Supporting Information

The in situ ^{13}C spectrum for β-cyclodextrin at 120 °C with x_w = 0.30 at 5 h, the time evolutions of the concentrations of the reactant and products for the reactions of α- and γ-cyclodextrins at 180 °C with x_w = 0.30, and the comparison of the D-fructose/D-glucose ratio between the D-maltose and the D-cellobiose reactions. This material is available free of charge via the Internet at http://pubs.acs.org.

■ AUTHOR INFORMATION

Corresponding Author

*K. Yoshida: phone, +81-88-656-7669; fax, +81-88-655-7025; e-mail, yoshida@chem.tokushima-u.ac.jp.

Notes

The authors declare no competing financial interest.

■ ACKNOWLEDGMENTS

This work is supported by the Grants-in-Aid for Scientific Research (No. 25410019) from the Japan Society for the Promotion of Science. K.Y. is grateful for the donations from the Takahashi Industrial and Economic Research Foundation, the Suzuki Foundation, the Salt Science Research Foundation, No. 1114, JGC-S Scholarship Foundation, and SEI group CSR foundation. M.N. is grateful to AGC, Limited for the financial support.

■ REFERENCES

(1) Kimura, H.; Nakahara, M.; Matubayasi, N. In Situ Kinetic Study on Hydrothermal Transformation of D-Glucose into 5-Hydroxymethylfurfural through D-Fructose with ^{13}C NMR. *J. Phys. Chem. A* **2011**, *115*, 14013−14021.

(2) Kimura, H.; Nakahara, M.; Matubayasi, N. Noncatalytic Hydrothermal Elimination of the Terminal D-Glucose Unit from Malto- and Cello-Oligosaccharides through Transformation to D-Fructose. *J. Phys. Chem. A* **2012**, *116*, 10039−10049.

(3) Kimura, H.; Nakahara, M.; Matubayasi, N. Solvent Effect on Pathways and Mechanisms for D-Fructose Conversion to 5-Hydroxymethyl-2-furaldehyde: In Situ ^{13}C NMR Study. *J. Phys. Chem. A* **2013**, *117*, 2102−2113.

(4) Kimura, H.; Yoshida, K.; Uosaki, Y.; Nakahara, M. Effect of Water Content on Conversion of D-Cellobiose into 5-Hydroxymethyl-2-furaldehyde in a Dimethylsulfoxide−Water Mixture. *J. Phys. Chem. A* **2013**, *117*, 10987−10996.

(5) Nakahara, M.; Wakai, C. Monomeric and Cluster States of Water Molecules in Organic Solvent. *Chem. Lett.* **1992**, *21*, 809−812.

(6) Nakahara, M.; Wakai, C. Effect of Solvent, Temperature, and Pressure on Hydrogen Bonding and Reorientation of Water Molecules. *J. Mol. Liq.* **1995**, *65/66*, 149−155.

(7) Wakai, C.; Nakahara, M. Attractive Potential Effect on the Self-Diffusion Coefficients of A Solitary Water Molecule in Organic Solvents. *J. Chem. Phys.* **1997**, *106*, 7512−7518.

(8) Sasaki, M.; Kabyemela, B.; Malaluan, R.; Hirose, S.; Takeda, N.; Adschiri, T.; Arai, K. Cellulose Hydrolysis in Subcritical and Supercritical Water. *J. Supercrit. Fluids* **1998**, *13*, 261−268.

(9) Sasaki, M.; Fang, Z.; Fukushima, Y.; Adschiri, T.; Arai, K. Dissolution and Hydrolysis of Cellulose in Subcritical and Supercritical Water. *Ind. Eng. Chem. Res.* **2000**, *39*, 2883−2890.

(10) Nagamori, M.; Funazukuri, T. Glucose Production by Hydrolysis of Starch under Hydrothermal Conditions. *J. Chem. Technol. Biotechnol.* **2004**, *79*, 229−233.

(11) Chheda, J. N.; Román-Leshkov, Y.; Dumesic, J. A. Production of 5-Hydroxymethylfurfural and Furfural by Dehydration of Biomass-Derived Mono- and Poly-Saccharides. *Green Chem.* **2007**, *9*, 342−350.

(12) Lin, Y.-C.; Cho, J.; Tompsett, G. A.; Westmoreland, P. R.; Huber, G. W. Kinetics and Mechanism of Cellulose Pyrolysis. *J. Phys. Chem. C* **2009**, *113*, 20097−20107.

(13) Liu, X.-X.; Yu, L.; Xie, F.-W.; Li, M.; Chen, L.; Li, X.-X. Kinetics and Mechanism of Thermal Decomposition of Cornstarches with Different Amylose/Amylopectin Ratios. *Starch/Stärke* **2010**, *62*, 139−146.

(14) Zheng, M.-Y.; Wang, A.-Q.; Ji, N.; Pang, J.-F.; Wang, X.-D.; Zhang, T. Transition Metal-Tungsten Bimetallic Catalysts for the Conversion of Cellulose into Ethylene Glycol. *ChemSusChem.* **2010**, *3*, 63−66.

(15) Zhao, S.; Cheng, M.-X.; Li, J.-Z.; Tian, J.-A.; Wang, X.-H. One Pot Production of 5-Hydroxymethylfurfural with High Yield from Cellulose by a Brønsted-Lewis-Surfactant-Combined Heteropolyacid Catalyst. *Chem. Commun.* **2011**, *47*, 2176−2178.

(16) Mayes, H. B.; Broadbelt, L. J. Unraveling the Reactions that Unravel Cellulose. *J. Phys. Chem. A* **2012**, *116*, 7098−7106.

(17) Abdullah, R.; Ueda, K.; Saka, S. Decomposition Behaviors of Various Crystalline Celluloses as Treated by Semi-Flow Hot-Compressed Water. *Cellulose* **2013**, *20*, 2321−2333.

(18) Chheda, J. N.; Huber, G. W.; Dumesic, J. A. Liquid-Phase Catalytic Processing of Biomass-Derived Oxygenated Hydrocarbons to Fuels and Chemicals. *Angew. Chem,. Int. Ed.* **2007**, *46*, 7164−7183.

(19) Rosatella, A. A.; Simeonov, S. P.; Frade, R. F. M.; Afonso, C. A. M. 5-Hydroxymethylfurfural (HMF) as a Building Block Platform: Biological Properties, Synthesis and Synthetic Applications. *Green Chem.* **2011**, *13*, 754−793.

(20) van Putten, R.-J.; van der Waal, J. C.; de Jong, E.; Rasrendra, C. B.; Heeres, H. J.; de Vries, J. G. Hydroxymethylfurfural, A Versatile Platform Chemical Made From Renewable Resources. *Chem. Rev.* **2013**, *113*, 1499−1597.

(21) van Putten, R.-J.; Soetedjo, J. N. M.; Pidko, E. A.; van der Waal, J. C.; Hensen, E. J. M.; de Jong, E.; Heeres, H. J. Dehydration of Different Ketoses and Aldoses to 5-Hydroxymethylfurfural. *ChemSusChem.* **2013**, *6*, 1681−1687.

(22) Choudhary, V.; Mushrif, S. H.; Ho, C.; Anderko, A.; Nikolakis, V.; Marinkovic, N. S.; Frenkel, A. I.; Sandler, S. I.; Vlachos, D. G. Insights into the Interplay of Lewis and Brønsted Acid Catalysts in Glucose and Fructose Conversion to 5-(Hydroxymethyl)furfural and Levulinic Acid in Aqueous Media. *J. Am. Chem. Soc.* **2013**, *135*, 3997−4006.

(23) Shi, N.; Liu, Q.-Y.; Zhang, Q.; Wang, T.-J.; Ma, L.-L. High Yield Production of 5-Hydroxymethylfurfural from Cellulose by High Concentration of Sulfates in Biphasic System. *Green Chem.* **2013**, *15*, 1967−1974.

(24) Dutta, S.; De, S.; Saha, B. Advances in Biomass Transformation to 5-Hydroxymethylfurfural and Mechanistic Aspects. *Biomass & Bioenergy* **2013**, *55*, 355−369.

(25) Gallo, J. M. R.; Alonso, D. M.; Mellmer, M. A.; Dumesic, J. A. Production and Upgrading of 5-Hydroxymethylfurfural Using Heterogeneous Catalysts and Biomass-Derived Solvents. *Green Chem.* **2013**, *15*, 85−90.

(26) Caes, B. R.; Palte, M. J.; Raines, R. T. Organocatalytic Conversion of Cellulose into a Platform. *Chem. Sci.* **2013**, *4*, 196−199.

(27) The standard specific combustion energy for D-glucose is 15.6 kJ g^{-1} (ref 28), whereas that for 5-HMF is 22.1 kJ g^{-1} (ref 29). The specific combustion energy density is thus enhanced by the formation of the unsaturated bonds due to the dehydration.

(28) Kabo, G. J.; Voitkevich, O. V.; Blokhin, A. V.; Kohut, S. V.; Stepurko, E. N.; Paulechka, Y. U. Thermodynamic Properties of Starch and Glucose. *J. Chem. Thermodynamics* **2013**, *59*, 87−93.

(29) Verevkin, S. P.; Emel'yanenko, V. N.; Stepurko, E. N.; Ralys, R. V.; Zaitsau, D. H.; Stark, A. Biomass-derived Platform Chemicals: Thermodynamic Studies on the Conversion of 5-Hydroxymethylfurfural into Bulk Intermediates. *Ind. Eng. Chem. Res.* **2009**, *48*, 10087−10093.